

Direct Electrodeposition of Tetrahexahedral Pd Nanocrystals with High-Index Facets and High Catalytic Activity for Ethanol Electrooxidation

Na Tian, Zhi-You Zhou, Neng-Fei Yu, Li-Yang Wang, and Shi-Gang Sun*

State Key Lab of Physical Chemistry of Solid Surfaces, Department of Chemistry, College of Chemistry and Chemical Engineering, Xiamen University, Xiamen 361005, China

Received March 15, 2010; E-mail: sgsun@xmu.edu.cn

The catalytic activity of nanoparticles is highly dependent on their surface structure, especially the density of low-coordinated surface atoms (such as atomic steps and kinks).¹ Open-structure surfaces (e.g., high-index planes for face-centered cubic lattice metals), which contain a high density of low-coordinated atoms, are generally superior in catalytic activity and stability to flat planes that are composed of closely packed surface atoms.² Therefore, the shape-controlled synthesis of nanocrystals (NCs) enclosed by open-structure surfaces is an exciting direction to pursue for significantly enhancing the NCs' catalytic activity and has attracted great interest in recent years.³ It is, however, a great challenge to synthesize NCs with open-structure surfaces because of their high surface energies.

We recently developed a shape-controlling electrochemical method for synthesizing tetrahexahedral (THH) Pt NCs enclosed by {730} and vicinal high-index facets.⁴ In this method, Pt nanospheres were first electrodeposited on a glassy carbon (GC) substrate, and then a square-wave potential treatment was applied to them, resulting in the growth of THH Pt NCs. This two-step method was also applied to the synthesis of trapezohedral Pd NCs with {hkk} facets and concave hexoctahedral Pd NCs with {hkl} facets.⁵ In addition, we produced fivefold twinned Pd nanorods (~2 μm in length) with high-index facets on a GC substrate in 5 mM PdCl₂ solution by using a square-wave potential method.⁶ However, THH Pd NCs with {hk0} high-index facets, which, like the THH Pt NCs, may also exhibit a high catalytic activity, could not be obtained by the above-mentioned methods. Although the synthesis of THH Au NCs was also reported recently,^{3b} the preparation of THH Pd NCs has not been successful to date.

In this communication, we report for the first time the direct electrodeposition of THH Pd NCs with {730} high-index facets using a programmed electrodeposition method we have developed. The as-prepared THH Pd NCs exhibit high catalytic activity toward ethanol electrooxidation in alkaline media.

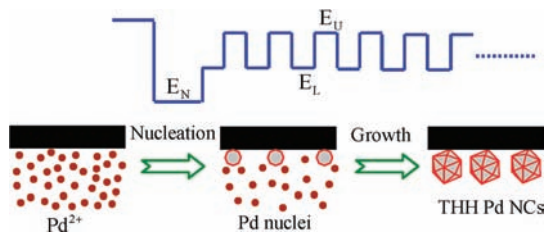


Figure 1. Illustration of the programmed electrodeposition method for preparation of tetrahexahedral Pd nanocrystals (THH Pd NCs).

THH Pd NCs were electrodeposited directly on a GC electrode in 0.2 mM PdCl₂ + 0.1 M HClO₄ solution by a programmed electrodeposition method, as illustrated in Figure 1. The GC electrode was first subjected to a potential step from 1.20 V (vs

SCE) to -0.10 V (E_N), and this potential was maintained for 20 ms to generate Pd nuclei. The growth of the Pd nuclei into THH Pd NCs was achieved by applying a square-wave potential ($f = 100$ Hz) with lower (E_L) and upper (E_U) potential limits of 0.30 and 0.70 V, respectively. This preparation method is simple and straightforward and avoids the coexistence of THH NCs with residual polycrystalline nanospheres, in comparison with the previous two-step method.⁴

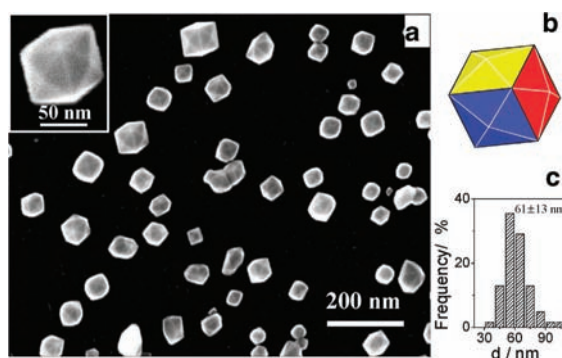


Figure 2. (a) SEM image of THH Pd NCs. The inset is a high-magnification SEM image. (b) Geometrical model of a tetrahexahedron. (c) Size histogram of THH Pd NCs. Preparation conditions: $E_N = -0.10$ V, $E_L = 0.30$ V, $E_U = 0.70$ V; 30 min growth time; 0.2 mM PdCl₂ + 0.1 M HClO₄.

Figure 2a shows an overview scanning electron microscopy (SEM) image of the THH Pd NCs. A THH polyhedron has 24 facets and can be identified as a cube with each face capped by a square-based pyramid, as shown by the model in Figure 2b. In the high-magnification SEM image (Figure 2a inset), three perfect square-based pyramids can be clearly observed, confirming that the Pd NC has a THH shape. The yield of the THH Pd NCs was over 80%, and the other shapes were an agglomeration of imperfect THH and irregular polyhedra. The average size of the THH Pd NCs was 61 nm (Figure 2c). The key for the successful preparation of THH Pd NCs consists of three aspects: (1) use of a dilute PdCl₂ solution, (2) employment of the nucleation potential E_N , and (3) the well-controlled square-wave potential. When the PdCl₂ concentration was increased from 0.2 to 1.0 mM, a lot of twinned Pd nanorods were produced (Figure S1 in the Supporting Information). When the nucleation step was skipped, Pd NCs hardly grew on the GC electrode in such a dilute PdCl₂ solution (Figure S2). More importantly, the formation of high-index facets on the Pd NCs is controlled by the dynamic interplay between the growth at E_L and surface reconstruction by moderate oxygen adsorption at E_U .⁵ It was found that the potential window for the growth of THH Pd NCs ranged from 0.25 to 0.35 V for E_L and from 0.65 to 0.75 V for E_U . For E_L and E_U outside these ranges, many irregular Pd nanoparticles were obtained (Figure S3).

The surface structure of the THH Pd NCs was determined by selected-area electron diffraction (SAED) and high-resolution transmission electron microscopy (HRTEM). Similar to the analysis of THH Pt NCs,⁴ we captured TEM images of Pd NCs along the [001] orientation, as shown in Figure 3a. In this orientation, eight side facets parallel to the [001] axis can be imaged edge-on and form an octagonal projection, as illustrated by the THH model shown in the Figure 3 inset. Clearly, the TEM image of the Pd NC is in good agreement with the model. Four imperfect vertices in the $\langle 100 \rangle$ direction were caused by the slight elongation of the THH shape.^{3b,4} A fourfold-symmetrical SAED pattern (Figure 3b) was obtained, confirming the single-crystalline structure of the THH Pd NC.

The Miller indices of exposed facets on the THH Pd NC were identified by careful measurement of crystal plane angles (i.e., α and β in the Figure 3 inset). In Figure 3a, the average α and β were measured to be 133 and 137°, respectively (Figure S4), which are close to the theoretical values ($\alpha = 133.6^\circ$, $\beta = 136.4^\circ$) for a THH NC with {730} facets.⁴ This result indicates that the dominant facets of the Pd THH NC are {730}. The {730} facet is periodically composed of two {210} steps followed by one {310} step. Figure 3c shows an HRTEM image recorded from the boxed area in Figure 3a. The continuous lattice fringes with lattice spacing of 0.20 nm, corresponding to the {200} planes of Pd, can be observed. Moreover, some {210} and {310} steps, as marked in Figure 3d, can be discerned on the border atoms, consistent with the atomic arrangement of {730} facets.

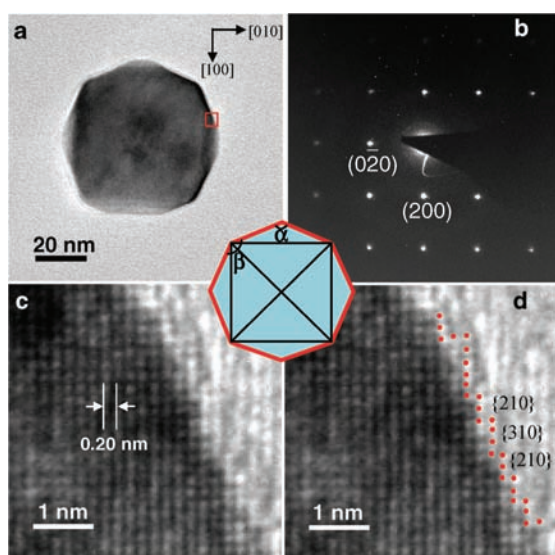


Figure 3. (a) TEM image of a THH Pd NC recorded along the [001] direction. The inset is a [001]-projected THH model. (b) SAED pattern. (c) HRTEM image recorded from the boxed area in (a), showing some {210} and {310} steps that have been marked in (d) for clarity.

Pd exhibits high catalytic activity toward ethanol electrooxidation in alkaline media, so this reaction was used as a test reaction to characterize the catalytic activity of the THH Pd NCs. Figure 4 depicts cyclic voltammograms of THH Pd NCs and commercial Pd black recorded in 0.1 M ethanol + 0.1 M NaOH solution. The oxidation current was normalized to the electroactive surface area, which was measured from the electric charge of hydrogen adsorption/desorption on Pd surfaces (Figure S5);⁷ this allowed the current density to be directly used to compare the catalytic activities of different samples. The peak current densities of ethanol oxidation

on the THH Pd NCs and Pd black catalyst were 1.84 and 0.42 mA cm⁻², respectively, in the positive-going potential scan; the corresponding values were 3.83 and 0.65 mA cm⁻² in the negative-going potential scan. The THH Pd NCs exhibited 4–6 times higher catalytic activity than commercial Pd black catalyst, which may be caused by the high density of surface atomic steps on THH Pd NCs. For catalytic activity per unit mass of Pd, our estimation indicates that the activity of THH Pd NCs is about 1.5–3 times that of the commercial Pd black (see the Supporting Information). In addition, the THH Pd NCs also exhibited high stability. After 1000 potential cycles, 95.5 and 75.0% of the initial catalytic activity in the positive- and negative-going potential scans, respectively, was still maintained (Figure S7).

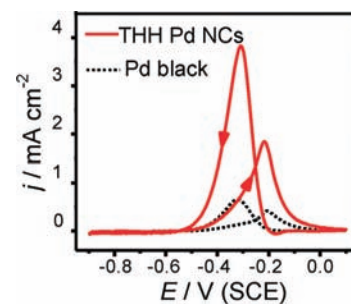


Figure 4. Cyclic voltammograms of THH Pd NCs (solid line) and Pd black catalyst (dashed line) at 10 mV s⁻¹ in 0.1 M ethanol + 0.1 M NaOH.

In summary, we have developed a programmed electrodeposition method to fabricate THH Pd NCs enclosed by {730} high-index facets. Thanks to their high density of surface atomic steps, the THH Pd NCs exhibited 4–6 times higher catalytic activity per unit surface area than a commercial Pd black catalyst toward ethanol electrooxidation. This simple and straightforward method is of significance for facile preparation of high-index-faceted metal nanocatalysts with high catalytic activity.

Acknowledgment. This study was supported by NSFC (20873113, 20933004, 20833005, and 20921120405), MOST (2007DFA40890), and Fujian Provincial Department of Science and Technology (2008F3099 and 2008I0025).

Supporting Information Available: Detailed materials, preparation, and characterization of THH Pd NCs. This material is available free of charge via the Internet at <http://pubs.acs.org>.

References

- (1) (a) Lim, B.; Jiang, M. J.; Camargo, P. H. C.; Cho, E. C.; Tao, J.; Lu, X. M.; Zhu, Y. M.; Xia, Y. N. *Science* **2009**, *324*, 1302. (b) Narayanan, R.; El-Sayed, M. A. *Nano Lett.* **2004**, *4*, 1343. (c) Lee, S. W.; Chen, S.; Sheng, W. C.; Yabuuchi, N.; Kim, Y. T.; Mitani, T.; Vescovo, E.; Shao-Horn, Y. *J. Am. Chem. Soc.* **2009**, *131*, 15669. (d) Zhou, Z. Y.; Huang, Z. Z.; Chen, D. J.; Wang, Q.; Tian, N.; Sun, S. G. *Angew. Chem., Int. Ed.* **2010**, *49*, 411.
- (2) (a) Somorjai, G. A.; Blakely, D. W. *Nature* **1975**, *258*, 580. (b) Somorjai, G. A. *Science* **1985**, *227*, 902. (c) Tian, N.; Zhou, Z. Y.; Sun, S. G. *J. Phys. Chem. C* **2008**, *112*, 19801.
- (3) (a) Ma, Y. Y.; Kuang, Q.; Jiang, Z. Y.; Xie, Z. X.; Huang, R. B.; Zheng, L. S. *Angew. Chem., Int. Ed.* **2008**, *47*, 8901. (b) Ming, T.; Feng, W.; Tang, Q.; Wang, F.; Sun, L. D.; Wang, J. F.; Yan, C. H. *J. Am. Chem. Soc.* **2009**, *131*, 16350.
- (4) Tian, N.; Zhou, Z. Y.; Sun, S. G.; Ding, Y.; Wang, Z. L. *Science* **2007**, *316*, 732.
- (5) Zhou, Z. Y.; Tian, N.; Huang, Z. Z.; Chen, D. J.; Sun, S. G. *Faraday Discuss.* **2008**, *140*, 81.
- (6) Tian, N.; Zhou, Z. Y.; Sun, S. G. *Chem. Commun.* **2009**, 1502.
- (7) Miyake, H.; Okada, T.; Samjeske, G.; Osawa, M. *Phys. Chem. Chem. Phys.* **2008**, *10*, 3662.

JA102177R